Membrane and Water Treatment, *Vol. 17, No. 2 (2026) 169-187*
https://doi.org/10.12989/mwt.2026.17.2.169

Treatment of kitchen wastewater with MWCNTs membranes: Impact of non-acidic oxidation and diameter

Alessandra Chew Fei Yee[1], Kah Chun Ho*[1,2,3], Jiun Hor Low[1,2,3]

[1]*School of Engineering, Faculty of Innovation and Technology, Taylor's University, No. 1, Jalan Taylor's, 47500, Subang Jaya, Selangor, Malaysia*
[2]*Clean Technology Impact Lab, Taylor's University, No.1, Jalan Taylor's, 47500, Subang Jaya, Selangor, Malaysia*
[3]*Centre for Sustainable Societies, Taylor's University, No.1, Jalan Taylor's, 47500, Subang Jaya, Selangor, Malaysia*

(Received June 26, 2025, Revised February 27, 2026, Accepted March 10, 2026)

Abstract. Massive amounts of kitchen wastewater mainly composed of organic colloidal matter is produced by the food service industry. In this study, the performance of nanocomposite membrane incorporated by multi-walled carbon nanotubes (MWCNTs) are evaluated. The effect of non-acidic oxidative reagents (NH_4OH: H_2O_2) and diameter of MWCNTs was studied. Membrane characterization including surface functional groups, porosity and pore size, surface hydrophilicity, and membrane morphology was conducted. The results showed that the higher NH_4OH/ H_2O_2 ratio (3:1) introduced more oxygen-containing functional groups on the oxidized MWCNTs (OMWCNTs). The large diameter of MWCNTs (20-30 nm) tend to produce nanocomposite membrane with bigger pore size and the oxidation of MWCNTs has further enhanced the membrane hydrophilicity. The highest membrane water permeability (245.50 L/m^2 h bar) was attained by nanocomposite membrane (M2c) modified by larger diameter OMWCNTs with higher NH_4OH/ H_2O_2 ratio (3:1). In terms of kitchen wastewater treatment, all nanocomposite membrane showed improved pollutant rejection for suspended solids (SS) (96.48-98.74%), turbidity (98.88-100%), color (61.54-66.67%), chemical oxygen demand (COD) (28.42-38.92%), and total dissolved solids (TDS) (3.57-36.70%). Besides, the M2c nanocomposite membrane showed the highest antifouling performance compared to other nanocomposite membranes. This enhancement was attributed to the increased surface negative charge and formation of loose foulant layer on the membrane surface.

Keywords: kitchen wastewater; multi-walled carbon nanotubes; MWCNTs diameter; nanocomposite membrane; non-acidic oxidation; wastewater treatment

1. Introduction

Rapid urbanization due to rise of population increased the scale of food service industry. The food preparation and consumption generated considerable amounts of kitchen wastewater which constitutes about 3% of urban domestic sewage discharge while its contents of chemical oxygen demand (COD) and biochemical oxygen demand (BOD) account for approximately 33% of the total load [1]. This is mainly due to the presence starch, food fibers, animal fats produced by food

*Corresponding author, Ph.D., E-mail: kahchun.ho@taylors.edu.my

ISSN: 2005-8624 (Print), 2092-7037 (Online)

processing. Kitchen wastewater composition varies significantly with the type of food served in the restaurant and it is mainly composed of organic colloidal matter, suspended solids, soap, and detergents. In general, kitchen wastewater contains high COD (4,000-145,000 mg/L), high suspended solids (800-185,000 mg/L), and total phosphorus (TP) (10-350 mg/L) [2].

Unlike developed countries, kitchen wastewater is typically directed to the sewage treatment plants via sewers; kitchen wastewater in developing countries is discharged directly into drains without proper on-site treatment often exacerbated by a lack of awareness [3]. Most often, kitchen wastewater containing high organic matter limits the operating load of sewage treatment systems, deteriorating the treatment plants performance. In addition, the fat and grease content of kitchen wastewater causes adhesion and deposition on sewage pipe network, and secondary pollution due to corrosion and acidification [4]. Besides, kitchen wastewater also produces biogas which poses potential safety hazard and foul odor in the pipeline system. Hence, a more sustainable method to rectify this issue is by pretreating the wastewater onsite prior releasing them into the sewers. Membrane-based separation processes have emerged as one of the most promising technologies for wastewater treatment due to their high contaminants removal efficiency and compact size. Al-Alawy and Al-Ameri [5] have reported more than 96% oil removal can be achieved by commercial hollow fiber ultrafiltration (UF) membrane in a pilot plant and the treated water can be reused in the process. However, the practical applications of membrane technology are greatly limited by fouling due to the blockage of membrane pores by organic matter. Frequent cleaning to restore membrane performance increases operating costs and decreases membrane lifespan [6].

To address this, researchers have explored various fouling mitigation strategies like pre-treatment, operating condition optimization, and membrane modification. Among these approaches, membrane or substrate modification using carbon-based nanomaterials has received significant attention due to their unique physicochemical properties, such as excellent chemical and mechanical stability, electrical conductivity, and reinforcement capability [7, 8]. Among these nanomaterials, membrane modification through the incorporation of multi-walled carbon nanotubes (MWCNTs) has also garnered considerable interest [9]. Studies have demonstrated that incorporating MWCNTs into membrane can improve nanocomposite membrane performance like pollutant removal, permeate flux and antifouling properties [10]. Additionally, MWCNTs have shown antibacterial effects, effectively eliminating pathogenic bacteria deposited on the membrane surface. Despite these advantages, the primary challenge in using MWCNTs is their tendency to agglomerate [11]. Therefore, introducing functional groups on MWCNTs through oxidation could increase their dispersion in solutions. Oxidation using acidic reagents (nitric acid and a mixture of sulfuric acid (H_2SO_4) and hydrogen peroxide (H_2O_2)) and basic reagents (ammonium hydroxide (NH_4OH)/H_2O_2) agents have been studied [12]. It is found that non-acidic oxidation using NH_4OH)/H_2O_2 is the most effective for impurities removal and mild oxidation of the MWCNTs. This is beneficial to retain most of inherent properties of MWCNTs with no appreciable structural damage [13]. In addition, the structure of MWCNTs plays an important role in the performance of nanocomposite membrane. It is reported that the diameter of MWCNTs could affect the dispersibility and interaction with the contaminants. Larger diameter of MWCNTs is observed to enhance the antifouling properties of nanocomposite membrane in treating dye wastewater with higher normalized flux due to the larger specific surface area hence higher surface repulsion force [14].

Nonetheless, there are limited studies that investigated the effect of non-acidic oxidative reagents and diameter of MWCNTs on the performance of nanocomposite membrane. It is hypothesized that the ratio of NH_4OH: H_2O_2 affects the oxidation potential of MWCNTs while the diameter of

Table 1. Membrane formulation and abbreviation

Membrane	Diameter of MWCNTs (nm)	Non-acidic oxidative reagents ratio (v/v)	
		NH_4OH	H_2O_2
M0	-	-	-
M1a	12-15	-	-
M1b	12-15	1	1
M1c	12-15	3	1
M2a	20-30	-	-
M2b	20-30	1	1
M2c	20-30	3	1

MWCNTs influences the surface area available for oxidation. This would affect the dispersibility and compatibility of MWCNTs within polymer matrices thereby membrane performance. Hence, this research aims to explore the influence of non-acidic oxidative reagents ratio (NH_4OH: H_2O_2) and diameter of MWCNTs on the characteristics and performance of nanocomposite membranes in treating the real kitchen wastewater.

2. Materials and methods

2.1 Materials

MWCNTs with two different diameters (12-15 nm, 20-30 nm) and purity greater than 97% were supplied by Ugent Tech, Malaysia and NanoAmor, USA, respectively. Polyvinylidene Fluoride (PVDF) T-1 from Shanghai Ofluorine Co., China while 99% purity Dimethylacetamide (DMAc) from Merck KGaA, Germany were used for membrane synthesis. 25% NH_4OH and 30% w/v H_2O_2 were obtained from Merck KGaA, Germany as non-acidic oxidative reagents. Lastly, real kitchen wastewater was obtained from the Taylor's Culinary Institute (TCI), Malaysia. To preserve the kitchen wastewater, the wastewater was kept at 4°C.

2.2 Oxidation of MWCNTs

Oxidation of MWCNTs was carried out using non-acidic oxidative reagents NH_4OH and H_2O_2 following the literature [13]. 0.3 g of MWCNTs were dispersed in 25 mL mixture of NH_4OH and H_2O_2. Ratio of NH_4OH: H_2O_2 was manipulated at 1:1 and 3:1 (v/v) [15]. The suspension was heated to 80°C and stirred for 5 hours. After it had cooled down to room temperature, the suspension was separated by a 0.45 μm hydrophilized polytetrafluoroethylene (PTFE) membrane. The solid residue was washed thoroughly with distilled water until the filtrate reaches neutral pH. The solid residue was dried in an oven at 80°C to obtain the oxidized MWCNTs (OMWCNTs).

2.3 Synthesis of nanocomposite membrane

MWCNTs nanocomposite membrane was prepared by direct blending method. In brief, 1 wt% of MWCNTs was added into DMAc and dispersed using ultrasonicator (P120H, Elmasonic,

Germany) at 80 kHz and 1330W for 30 minutes [14]. Then, 18 wt% of PVDF powder was added to the nanomaterial suspension [16]. The membrane polymer solution was stirred at 250 rpm and 65°C for 4 hours followed by 40°C for an additional 3 hours to ensure the PVDF fully dissolves in the mixture. To remove any trapped air bubbles, the membrane polymer solution was left in a desiccator overnight. Next, 25 mL of the membrane polymer solution was poured onto a flat non-woven polyester membrane support (CU414 Opti, Neenah, US) secured on glass plate and spread evenly using a glass rod. The glass plate with the membrane polymer thin film was then submerged in a 5 L distilled water bath for one day to allow complete solidification. Finally, the synthesized membrane was removed from the water bath and stored in fresh distilled water at 4°C [17]. Table 1 shows the membrane formulation studied in this paper and its abbreviation.

2.4 Membrane characterization

2.4.1 Surface functional groups

The functional groups present on the surface of the nanocomposite membrane were determined by attenuated total reflectance-Fourier Transform Infrared Spectrometer (ATR-FTIR) using Thermo Scientific Nicolet Summit × FTIR Spectrometer, USA. A small piece of the membrane was placed on the crystal of the scanning area and the metal tip was pressed against the crystal to fix the sample. The wavelength range between 4000 cm^{-1} and 400 cm^{-1} was used to scan the sample.

2.4.2 Porosity and pore size

The gravimetric method was used to determine the porosity of the membrane while Guerout-Elford-Ferry equation was used to determine the membrane pore size [18]. Firstly, the membrane was soaked in distilled water for 12 hours to fill the pores with water. Following that, the wet membrane was cut into small pieces measuring 1 × 1 cm where it was weighed. Then, the membrane was dried at a temperature of 50°C for one whole day to remove excess water. The dried membrane was weighed again. The membrane thickness was measured by a thickness gauge. Membrane porosity and membrane pore size in terms of pore radius are calculated by Eq. (1) and Eq. (2), respectively [19].

$$\varepsilon = \frac{\frac{\omega_1 - \omega_2}{\rho_\omega}}{\frac{\omega_1 - \omega_2}{\rho_\omega} + \frac{\omega_2}{\rho_p}} \text{x } 100\% \tag{1}$$

where ε is membrane porosity (%), ω_1 and ω_2 are wet and dry weight of the membrane (g), respectively, ρ_ω and ρ_p is density of water (0.998 g/mL) and density of polymer (PVDF = 1.765 g/mL at 25°C), respectively.

$$r_m = \sqrt{\frac{(2.9 - 1.75\varepsilon)8V\mu\delta}{\varepsilon PA}} \tag{2}$$

where r_m is mean of membrane pore radius (m), V is water flow rate in (m^3/s), μ is dynamic viscosity of water at 25°C (0.891 mPa.s), δ is membrane thickness (m), ε is membrane porosity (%), P is operating pressure (Pa), A is membrane area (m^2).

2.4.3 Surface hydrophilicity

The surface hydrophilicity of membranes was assessed by water contact measurement using a contact angle goniometer (OCA 15Pro, DataPhysics Instruments, Germany) via the sessile drop method. 0.5 mL of distilled water droplet was gently dispensed on the membrane surface and at least 10 measurements were conducted to yield an average value.

2.4.4 Membrane morphology

The top surface and cross-sectional morphologies of the membranes were examined by using Scanning Electron Microscope (Hitachi TM3000, Tokyo, Japan). To examine the surface morphology, a membrane sample of 0.5 cm × 0.5 cm was cut and observed. For cross-sectional morphologies, membrane samples were submerged in liquid nitrogen and snapped to obtain clean cross-section view.

2.5 Kitchen wastewater characterization

2.5.1 Chemical oxygen demand (COD)

The COD of the kitchen wastewater was analyzed by chromosulfuric acid oxidation method. 3 mL of kitchen wastewater was added to a low-range COD digestion reagent vial (25 to 1500 mg/L) and the sample mixture was vigorously mixed. It was then heated at 148°C for 2 hours in a thermoreactor (Eco 8, VELP Scientifica Srl, Italy) and was left to cool to room temperature. After cooling, the sample mixture was measured using the UV/VIS spectrophotometer (Spectroquant® Prove 300, Merck, Germany) [20].

2.5.2 Suspended solid (SS)

The SS of the kitchen wastewater sample was analyzed using the UV/VIS spectrophotometer (Spectroquant® Prove 300, Merck, Germany). The kitchen wastewater sample was transferred into a 20 mm sample cell and was placed into the cell compartment. Distilled water was used as a blank [20].

2.5.3 Turbidity

The turbidity of the kitchen wastewater sample was analyzed by nephelometric method using a turbidity meter (TN-100, Eutech Instruments, Singapore). Approximately 10 mL of kitchen wastewater was placed into a sample cell and measured. Distilled water was used as a blank [21].

2.5.4 Total dissolved solid (TDS)

The TDS of the kitchen wastewater sample was analyzed using TDS meter (CON 2700, Eutech Instruments, Singapore). The TDS probe was rinsed with distilled water and then submerged in the kitchen wastewater until a stable measurement was obtained [22].

2.5.5 Color

The color of the kitchen wastewater sample was analyzed using UV/VIS spectrophotometer (Spectroquant® Prove 300, Merck, Germany) in accordance with ASTM D6045. The kitchen wastewater was transferred into 10 mm cell and was placed into the cell compartment. Zero cells were used as a blank [20].

2.5.6 pH

The pH of the kitchen wastewater sample was analyzed using a microprocessor pH meter (pH

211, Hanna Instruments, South Africa). The pH probe was rinsed with distilled water and then submerged in the kitchen wastewater until a stable measurement was obtained [23].

2.6 Membrane performance

Membrane filtration cell (16249, Sartorius Stedim Biotech, Germany) was utilized to evaluate the performance of the membrane at room temperature. The dead-end membrane filtration cell has a capacity of 200 mL and pressurized using compressed air. The filtration cell was used to evaluate the permeability of pure water, rejection as well as the fouling study towards kitchen wastewater. Prior to the experiment, the membranes were cut into a disc with a diameter of 47 mm and effective filtration area of 13 cm^2 [24].

2.6.1 Pure water permeability

To reduce the impact of compaction, the membranes were pre-pressurized at a constant pressure of 3 bar for 30 minutes until constant flux. The permeation flux was measured by filtering distilled water at varying transmembrane pressures (TMP) of 1.0, 1.5 and 2.0 bar, calculated using Eq. (3) [25]. Membrane permeability was determined from the slope of the permeation flux plotted against the TMP.

$$J = \frac{\Delta V}{A \Delta t} \tag{3}$$

where J is permeate flux (L m^{-2} h^{-1}), ΔV is permeate volume (L), A is effective surface area (m^2) and Δt is permeation time (h).

2.6.2 Kitchen wastewater rejection

The effectiveness of membrane was evaluated by using real kitchen wastewater as membrane feed solution. The physical properties (color, SS, TDS, turbidity, and pH) and chemical properties (COD) of the permeate were analyzed following procedures in Section 2.5. Initially, 200 mL of kitchen wastewater was added into the membrane filtration cell. The membrane rejection for each parameter was determined at a constant pressure of 2 bar and room temperature. By using Eq. (4), the rejection for each parameter was calculated [26].

$$R = \left(1 - \frac{C_p}{C_f}\right) x\ 100 \tag{4}$$

where R is rejection (%), C_p is treated kitchen wastewater and C_f is untreated kitchen wastewater.

2.6.3 Kitchen wastewater fouling study

The fouling behavior of the synthesized membranes for treating kitchen wastewater was evaluated by monitoring the normalized flux over a 30-minute filtration period at a constant pressure of 2 bar and room temperature [27]. The normalized flux was calculated using Eq. (5).

$$Normalized\ Flux = \frac{J_1}{J} \tag{5}$$

where J_1 is kitchen wastewater flux and J is distilled water flux.

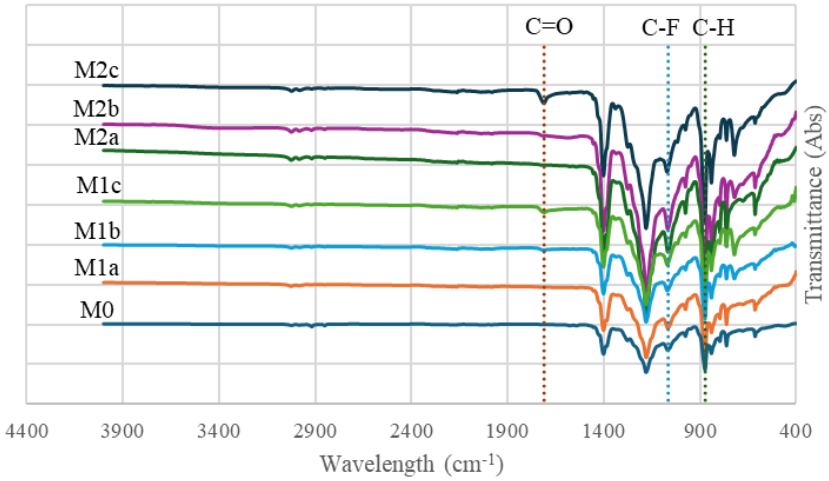

Figure 1. Surface functional groups present on the surface of the membranes

Table 2. Porosity, mean pore radius, and contact angle of membranes

Membrane	Porosity, ε (%)	Mean Pore Radius, r_m (nm)	Contact angle (°)
M0	64.32 ± 13.23	25.97 ± 4.49	More than 90
M1a	45.29 ± 23.79	12.26 ± 7.38	77.16 ± 0.57
M1b	22.56 ± 13.64	25.58 ± 15.44	78.19 ± 2.06
M1c	43.06 ± 5.71	40.60 ± 3.84	76.85 ± 0.54
M2a	55.50 ± 2.96	28.90 ± 1.16	71.03 ± 1.29
M2b	23.91 ± 2.96	67.80 ± 3.34	64.99 ± 1.61

3. Results and discussion

3.1 Membrane characterization

3.1.1 Surface functional groups

Fig. 1 shows the surface functional groups present on the surface of the membranes. As seen, all the membranes showed absorption peaks at 872 cm^{-1} and 1067 cm^{-1} for C-H bending and C-F stretching vibration [28]. Nevertheless, there is absence of two dominant peaks at 3550 cm^{-1} and 3670 cm^{-1} by -OH bond stretching vibration on nanocomposite membranes M1b, M1c, M2b, and M2c due to the incorporation of OMWCNTs [29]. This could be due to the low covalent functionalization of MWCNTs by non-acidic oxidation. This is in accordance with the literature where MWCNTs treated by non-acidic oxidative reagents NH_4OH/ H_2O_2 have relatively low amount of surface oxygen and milder damages of the graphitic sidewalls [13]. Nonetheless, absorption peak at 1710 cm^{-1} which is assigned to the C=O stretching was observed on nanocomposite membranes M1c and M2c. This is due to the higher degree of oxidation attributed by higher NH_4OH/ H_2O_2 ratio (3:1) which introduced more carboxyl functional groups on the carbon nanotubes skeleton [30].

3.1.2 Porosity, pore size and surface hydrophilicity

Table 2 shows the porosity, mean pore radius, and contact angle of membranes. As seen, the porosity of nanocomposite membranes decreased after the addition of MWCNTs and OMWCNTs. This could be due to the high density of nanomaterials in membrane at concentration of 1 wt%. This causes a portion of nanomaterials to aggregate irregularly in the membrane matrix during phase-inversion hence reduce the porosity. This is reported by Shah and Murthy [31] where high MWCNTs concentration (above 1 wt%) will cause aggregation of MWCNTs by van der Waals forces. The agglomerated nanomaterials connect porous regions and make the matrix more compact. In general, the nanocomposite membranes show membrane pore radius ranging from 12.26 nm to 79.24 nm which can be categorized as UF membrane suitable for COD and turbidity removal in the treatment of restaurant wastewater [3]. Additionally, it is observed that the nanocomposite membranes incorporated by MWCNTs with larger diameter of 20-30 nm (M2a, M2b, M2c) display larger pore radius as compared to that of small diameter of 12-15 nm (M1a, M1b, M1c). This is consistent with result obtained by Kah Chun et al. [14] where the MWCNTs with smaller diameters tend to agglomerate and reduced the pore size of membranes. The smaller diameter MWCNTs have larger effective interfacial contact area with the membrane matrix for the same concentration compared to the larger diameter MWCNTs. Besides, smaller diameter MWCNTs are more prone to hold together in entanglements owing to their large specific surface area, which results in strong Van der Waals forces among MWCNTs [32]. Besides, the nanocomposite membranes incorporated with OMWCNTs (M1b, M1c and M2b, M2c) exhibited higher pore size increment of 108.64-231.08% as compared to the MWCNTs (M1a and M2a) due to the increased functional groups on the membrane surface as evidenced by ATR-FTIR. Particularly, nanocomposite membranes with OMWCNTs treated by higher NH_4OH/ H_2O_2 ratio (3:1) showed highest increment of pore size due to the abundance of oxygen-containing functional groups. This speeds up the phase inversion process during membrane formation hence forming membrane with larger macro-voids [33].

As compared to M1c nanocomposite membrane blended with smaller diameter OMWCNTs, the M2c nanocomposite membrane with larger diameter OMWCNTs produced lower porosity but higher pore radius. This can be explained by the increased hydrophilicity of the membrane polymer solution. As presented in Fig. 1, the larger diameter of OMWCNTs poses more carboxyl functional groups which facilitate water diffusion while maintaining the outflow rate of DMAc solvent during membrane fabrication. This subsequently led to the creation of more pores with smaller sizes hence resulting in an enhanced porous structure consistent with other literature [34, 35].

In terms of surface hydrophilicity, the pristine PVDF M0 membrane shows contact angle more than 90^o which is slightly hydrophobic due to its low surface energy by fluorinated chemical structure [36]. The addition of OMWCNTs into the PVDF membrane matrix has increased the membrane surface hydrophilicity slightly to 64.99-78.19^o. The minimum changes on surface hydrophilicity could be due to the hydrophobic nature of MWCNTs and low oxidation degree by the non-acidic oxidative reagents NH_4OH/ H_2O_2. However, it should be pointed out that the membrane surface hydrophilicity is affected by many factors including chemistry and morphology in micro and macro scales [37].

3.2 Membrane performance

3.2.1 Pure water permeability

Fig. 2 shows the pure water permeability of membranes. As seen, most of the nanocomposite

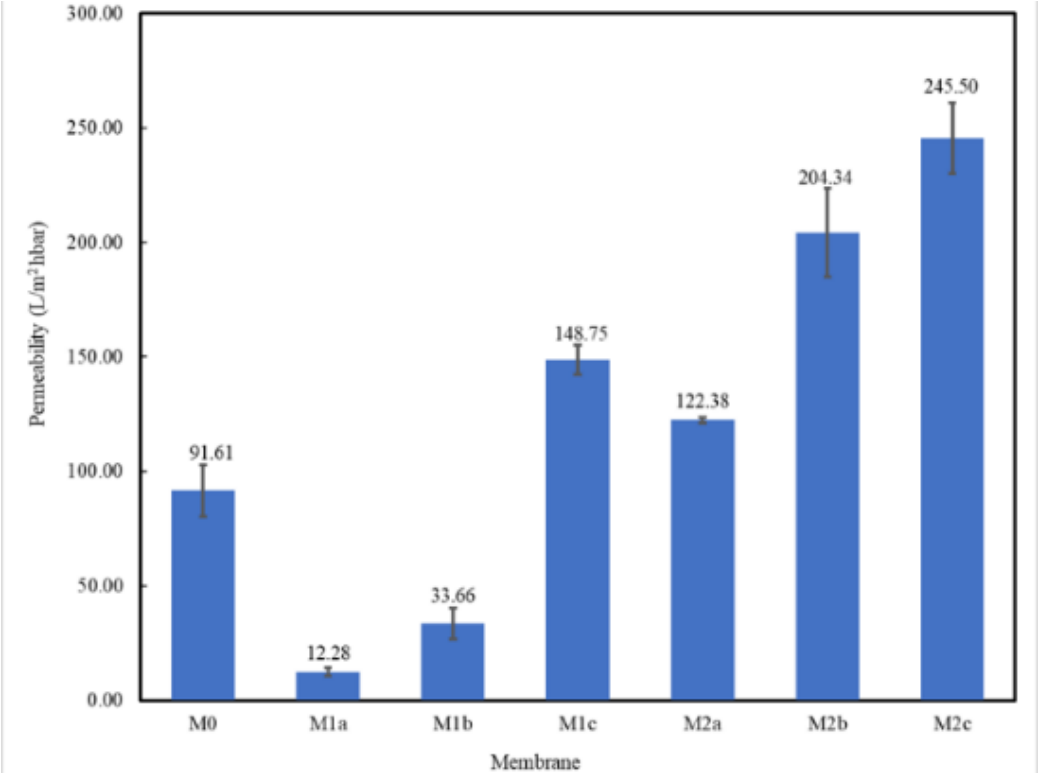

Figure 2. Pure water permeability of membranes

membranes incorporated with smaller diameter of MWCNTS (M1a and M1b) show lower water permeability than that of pristine PVDF membrane (M0). On the other hand, the nanocomposite membrane incorporated with larger diameter of MWCNTs (M2a, M2b, M2c) show increment of pure water permeability of 33.59%, 123.06%, and 167.98%, respectively, as compared to pristine PVDF membrane (M0). This result is consistent with the membrane pore size tabulated in Table 2 where the nanocomposite membrane incorporated with larger diameter of MWCNTs (M2a, M2b, M2c) have larger pore size. The larger membrane pore size allows faster water diffusion through the pores hence higher water permeability [38].

This is also evidenced by membrane surface morphology as shown in Fig. 3(a) and Fig. 3(b). As seen from the membrane surface, pristine PVDF membrane (M0) has smaller pore size and is more porous compared to the M2c nanocomposite membrane. Besides, the distribution of pore sizes also significantly affects water flow behavior. Wide pore-size distributions restrict water flow due to the presence of smaller pores, leading to decreased permeability [39]. The results are also consistent with data obtained by Chen et al. [40]. The increment of the pore size in nanocomposite membrane is attributed to the incorporation of nanomaterials that effectively enhance the transfer rate between the solvent and the nonsolvent. For the membrane cross-sectional view, M0 membrane presented a typical asymmetric structure consisting of finger-like pores across the membrane matrix.

As compared to the pristine membrane (M0), the OMWCNTs formed interspersed fluffy structure which could minimize the membrane thickness (Fig. 3(d) inset picture). This resulted in

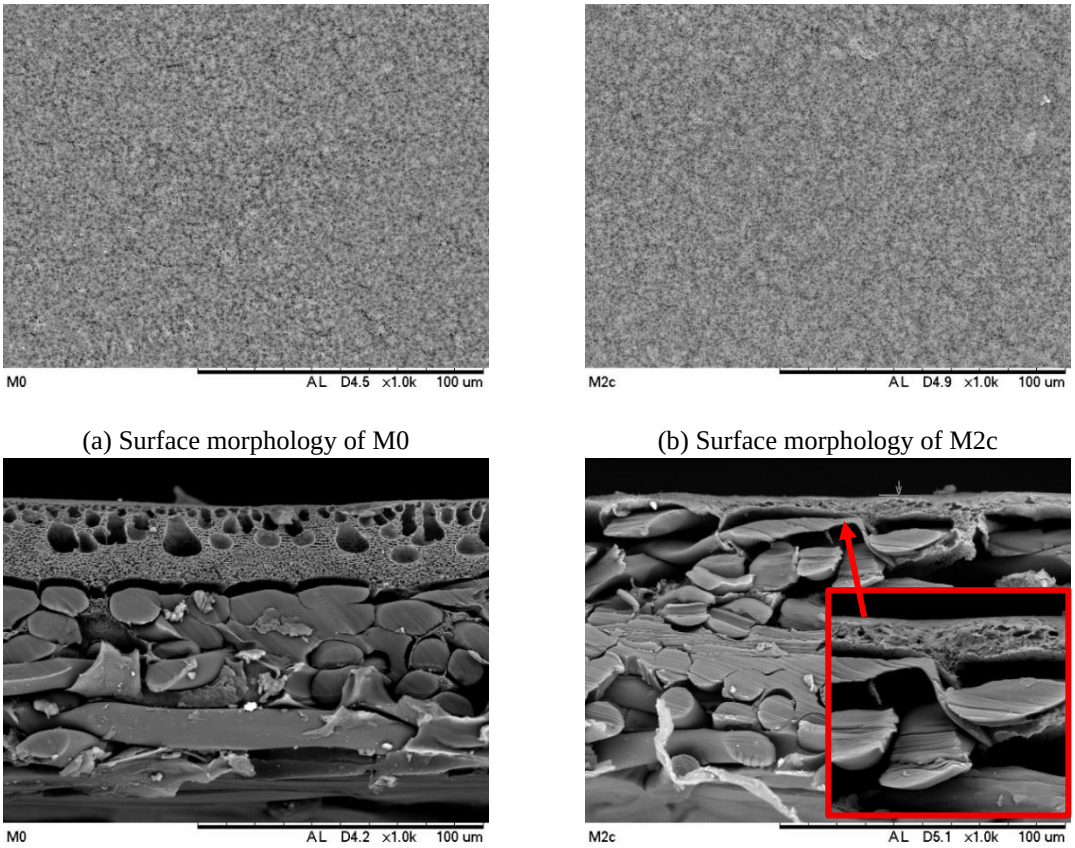

(a) Surface morphology of M0 (b) Surface morphology of M2c

(c) Cross-sectional view of M0 (d) Cross-sectional view of M2c

Figure 3. Surface morphology and cross-sectional view of M0 and M2c membranes at magnification of ×1.0 k

lower membrane resistance hence high pure water permeability which is consistent with the permeability result (Fig. 2). This is also in accordance with the study reported by Silva et al. [41] by blending different concentrations (1.0 to 6.7%) of MWCNTs into polydimethylsiloxane membranes for gas separation. The membrane thickness has decreased from 204 mm to 142 mm due to the formation of highly entwined structure of polymer and MWCNT resulting in a thinner membrane. This thin membrane layer shortens the effective transport path hence higher water permeability.

3.2.2 Kitchen wastewater rejection

As reported in Section 3.2.1, the nanocomposite membrane incorporated with MWCNTs with larger diameter (M2a, M2b and M2c) showed enhanced pure water permeability compared to pristine PVDF membrane (M0). Hence, these nanocomposite membranes were further evaluated for pollutant rejection and antifouling performance using real kitchen wastewater. The characteristics of raw and treated kitchen wastewater by membranes are summarized in Table 3. The raw kitchen wastewater contains moderate COD, SS and turbidity due to the presence of organic substances, oils, salts, and residual solid waste. These pollutants composition is generally

Table 3. Characteristics of raw and treated kitchen wastewater by membranes

Parameters	Raw kitchen wastewater	M0	M2a	M2b	M2c
COD (mg/L)	395.67-986.33	867.33	378.00	365.00	241.67
SS (mg/L)	142.00-148.67	107.67	5.00	5.00	5.00
Turbidity (NTU)	18.42-64.57	39.27	0.65	0.18	0
TDS (ppm)	56.00-72.67	55.67	50.67	48.00	46.00
Color (ASTM)	1.30-1.5	1.00	0.50	0.50	0.50
pH	4.27-4.35	4.38	7.09	7.30	7.57

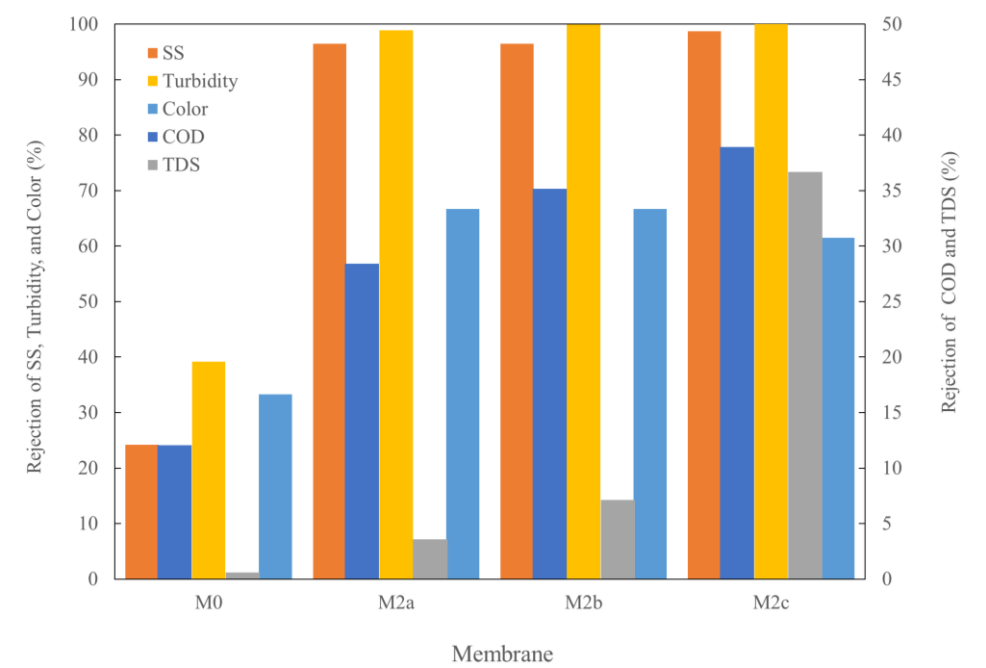

Figure 4. Membrane rejection on physical and chemical parameters of kitchen wastewater

lower than the typical kitchen wastewater reported by Li et al. [2] could be due to the types of kitchen processing facility. Fig. 4 shows the rejection of physical properties (color, SS, TDS, turbidity) and chemical properties (COD) of the kitchen wastewater by the synthesized membranes. The pristine M0 membrane showed relatively poor removal for SS (24.18%), turbidity (39.18%), color (33.33%), COD (12.06%), and TDS (0.6%). The lowest removal of TDS was due to the nature of UF membranes fabricated in this study which are not ideal to remove dissolved organics and fine organic components effectively [43]. On the other hand, comparatively higher removal was reported for SS and turbidity as the oils and animal fats particles in the kitchen wastewater are significantly larger than the pores size of the UF membranes. Therefore, their removal via size exclusion was highly effective [44]. This is also evident in the great reduction of colour and turbidity in the treated kitchen wastewater as shown in Fig. 5.

Upon the addition of MWCNTs/OMWCNTs, the nanocomposite membranes (M2a, M2b and M2c) exhibited better removal in terms of SS (96.48-98.74%), turbidity (98.88-100%), color

Figure 5. Picture of raw kitchen wastewater (left), treated kitchen wastewater (middle), and fouled membrane (right) [42]

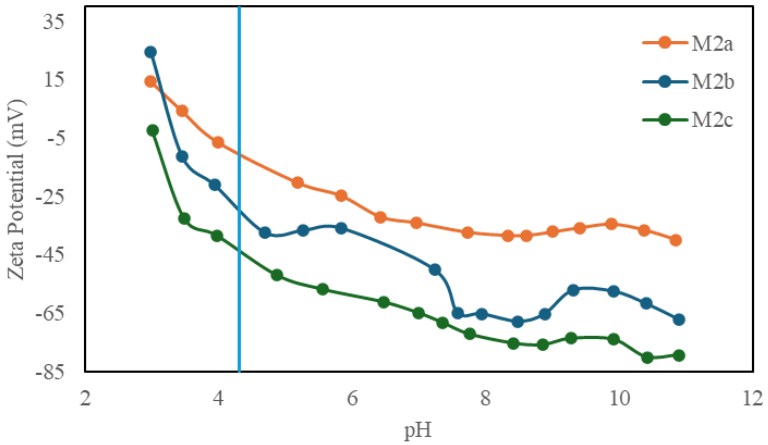

Figure 6. Surface charge of the nanocomposite membranes

(61.54-66.67%), COD (28.42-38.92%), and TDS (3.57-36.70%) compared to the pristine M0 membrane. This is contradictory with the larger pore radius in the nanocomposite membranes (28.90-79.24 nm) compared to the pristine PVDF M0 membrane (25.97 nm) as shown in Table 2. This significant improvement in rejection could be due to the formation of fouling layer by high membrane permeability in the nanocomposite membranes. The high membrane permeability could induce permeation drag that leads to the rapid particle deposition onto membrane to form fouling layer [45]. This can be evidenced by the cake layer on the fouled membrane shown in Fig. 5 (right). The fouling layer improved the rejection of large molecular pollutants in kitchen wastewater by steric exclusion mechanism [46]. This is also supported by Chang et al. [47] who assessed the relationship between solute rejection and membrane fouling. The study reported the high COD rejection is in close association with the cake layer deposition over the membrane. The organic solute can be removed by sieving/adsorption onto the cake layer that has been formed over the membrane surface.

Besides, the high pollutant removal using kitchen wastewater by the nanocomposite membranes could be explained through electrostatic repulsion. Fig. 6 shows the membrane surface charge

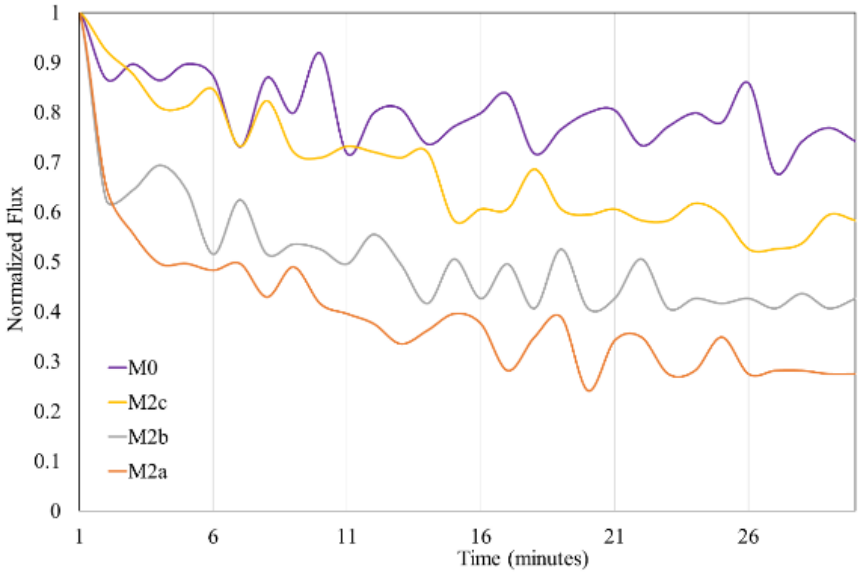

Figure 7. Normalized flux of pristine membrane and nanocomposite membranes

from pH 3 to pH 11. As the pH of kitchen wastewater ranged from 4.27 to 4.35, the measured surface charge of the M2a, M2b and M2c nanocomposite membranes are approximately -12.5 mV, -31.5 mV, and -44.5 mV. The acidic kitchen wastewater is attributed to the organic acids produced from the biodegradation of food waste [48]. As the MWCNTs are oxidized by non-acidic oxidative reagents NH_4OH and H_2O_2, chemical functional groups like carboxylates are added on the surface of MWCNTs. The functional groups imparted negative charges on the surface which enhanced the stability of OMWCNTs in solution. Pandey et al. [49] reported zeta potential for MWCNTs is −8.34 mV while for OMWCNTs oxidized by non-acidic reagents NH_4OH: H_2O_2 in the ratio 1:1 (v/v) is −21.2 mV. This is due to the attachment of negatively charged functional groups on the surface of MWCNTs. The addition of OMWCNTs into the membrane matrix subsequently increased the negative surface charge of the nanocomposite membrane which is evident in this study. The negatively charged membrane produces larger electrostatic repulsion between membranes and negatively charged pollutants [14]. This developed a loosely bound foulant layer can repel the negatively charged pollutants which will improve the filtration efficiency in the kitchen wastewater treatment [50]. To sum up, due to the complex pollutants composition in kitchen wastewater as shown in Table 3, the pollutant rejection mechanism was best explained by the (1) size exclusion either by membrane pores or the cake layer as well as (2) charge exclusion by the negatively charged membrane surface [51].

3.2.3 Kitchen wastewater fouling study

Fig. 7 shows the normalized flux of pristine PVDF membrane (M0) and nanocomposite membranes (M2a, M2b, and M2c) in 30 minutes of kitchen wastewater filtration. As seen, M0 membrane has the highest normalized flux (0.741) as compared to M2a (0.275), M2b (0.426) and M2c (0.583) at the end of filtration. This could be due to the lower water permeability of M0 membrane compared to the nanocomposite membranes as presented in Section 3.2.1. For the nanocomposite membrane, the higher permeate velocity (by 33.59-167.98%) at the membrane

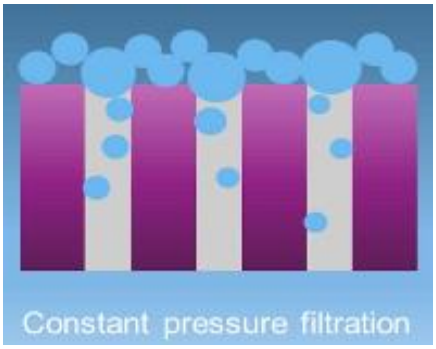

Figure 8. Fouling mechanisms at constant pressure [42]

pore leads to the greater drag forces across the membrane. Therefore, pollutants in the kitchen wastewater with smaller particle size tend to migrate more easily into the membrane pore hence caused severe reduction in permeate flux. This observation is consistent with Alborzi et al. [52] study relating flux decline with molecular weight cut-off (MWCO). The rate of flux decline is significantly higher for the membrane with 500 kDa MWCO while membranes with 10 kDa and 100 kDa MWCO displayed almost similar rates of flux decline. This validated that the membranes with high MWCO or large pore size tend to experience rapid fouling.

Nevertheless, it is observed the M2c nanocomposite membrane has higher normalized flux compared to the M2a and M2b despite the highest water permeability. This is attributed to the highest negative surface charge of M2c nanocomposite membrane. The negative surface charge creates strong repulsive electrostatic force with negatively charged foulants thus preventing them from entering the membrane pores. However, due to the high-water permeability and large membrane pore size of M2c nanocomposite membranes (Fig. 2 & Table 2), the foulants readily enter the membrane pores causing standard pore blocking and complete pore blocking (Fig. 8). These fouling mechanisms are more challenging for membrane flux recovery due to internal pore blocking despite the intrinsic membrane negative surface charge [42]. Hence, membrane backwashing and chemical cleaning are recommended for effective flux recovery. In general, the antifouling mechanism for nanocomposite membranes was mainly due to the favorable changes in membrane hydrophilicity, surface roughness, and surface charge [53]. However, these factors may not fully explain the antifouling mechanism in this study, as kitchen wastewater contains various pollutants that lead to complex pollutant-membrane interactions in real wastewater [54, 55].

In summary, M2c nanocomposite membrane stands out as the most optimal membrane which has the highest water permeability, improved pollutant rejection and good antifouling properties among all the nanocomposite membranes for kitchen wastewater treatment.

4. Conclusions

In conclusion, this study investigated the effect of non-acidic oxidative reagents and diameter of MWCNTs on the performance of nanocomposite membrane for kitchen wastewater treatment. The volume ratio of NH_4OH: H_2O_2 varied at 1:1 and 3:1 while the two different diameters of MWCNTs (12-15 nm, 20-30 nm) were studied. The results showed that non-acid oxidation imparts minute amount of surface oxygen and milder damage to the sidewalls of OMWCNTs.

While higher NH_4OH: H_2O_2 ratio of 3:1 introduced more oxygen-containing functional groups on the carbon nanotubes skeleton which could enhance the membrane hydrophilicity. In general, the addition of MWCNTs/OMWCNTs into the nanocomposite membrane enhanced the membrane characteristics such as bigger membrane pore size and compact membrane due to the formation of highly entwined structure of polymer and MWCNTs/OMWCNTs. Particularly, nanocomposite membrane (M2a, M2b, M2c) blended with larger diameter of MWCNTs/OMWCNTs yield a better performance in terms of water permeability and rejection. The nanocomposite membrane exhibited an increase in pure water permeability by 1.34-2.68-fold compared to the pristine PVDF membrane (M0), due to its larger pore size and thinner membrane layer. In terms of kitchen wastewater pollutant rejection, the nanocomposite membranes also exhibited higher rejection in terms of SS (96.48-98.74%), turbidity (98.88-100%), color (61.54-66.67%), COD (28.42-38.92%), and TDS (3.57-36.70%). The improvement was attributed to the stronger electrorepulsion and formation of loose foulant layer on membrane surface. Though, the nanocomposite membranes displayed higher fouling propensity due to the high water drag force resulting in rapid membrane pore or surface blocking. The nanocomposite membrane blended with larger diameter of OMWCNTs and higher NH_4OH: H_2O_2 (3:1) produced a comparable normalized flux (0.5829) with the pristine PVDF M0 membrane (0.7411). Future study should investigate the concentration of MWCNTs in the membrane matrix to optimize the overall performance of nanocomposite membranes. Besides, integrated wastewater treatment system should be adopted to pretreat the real kitchen wastewater prior to the membrane system to reduce the fouling propensity.

Acknowledgements

The authors wish to gratefully acknowledge the financial support by Taylor's University through Taylor's Internal Research Grant Scheme - Impact Lab Grant (TIRGS-ILG) (Project Code: TIRGS-ILG/2/2024/SOE/001 and TIRGS-ILG/1/2023/SOE/002). Appreciation to the Taylor's Culinary Institute (TCI), Malaysia for the supply of real kitchen wastewater.

References

1. Filimonau, V., Zhang, H., Wang, L. (2020). Food waste management in Shanghai full-service restaurants: A senior managers' perspective. Journal of Cleaner Production, 258, 120975. https://doi.org/10.1016/j.jclepro.2020.120975.
2. Li, W., Liu, H., Deng, L., Zhang, Y., Ma, Y., Chen, Y. (2024). Recent advances in treatment refinement of kitchen digested wastewater: feasibility, prospects, and technicalities. Water Cycle, 5, 20-30. https://doi.org/10.1016/j.watcyc.2023.12.001.
3. Zulaikha, S., Lau, W.J., Ismail, A. F., Jaafar, J. (2014). Treatment of restaurant wastewater using ultrafiltration and nanofiltration membranes. Journal of Water Process Engineering, 2, 58-62. https://doi.org/10.1016/j.jwpe.2014.05.001.
4. Yusuf, H. H., Roddick, F., Jegatheesan, V., Gao, L., Pramanik, B.K. (2023). Tackling fat, oil, and grease (FOG) build-up in sewers: insights into deposit formation and sustainable in-sewer management techniques. Science of The Total Environment, 904, 166761. https://doi.org/10.1016/j.scitotenv.2023.166761.
5. Al-Alawy, A.F., Al-Ameri, M.K. (2017). Treatment of simulated oily wastewater by ultrafiltration and nanofiltration processes. Iraqi Journal of Chemical and Petroleum Engineering, 18(1), 71-85. https://

doi.org/10.31699/IJCPE.2017.1.6.
6. Lv, Z., Zhang, S., Jiao, W., Zuo, X., Zhang, Y., Liu, Y. (2023). High-efficiency cleaning technology and lifespan prediction for the ceramic membrane treating secondary treated effluent. Water Science & Technology, 88(1), 321-338. https://doi.org/10.2166/wst.2023.209.
7. Cheong, K.L., Pang, M.M., Low, J.H., Tshai, K.Y., Koay, S.C., Wong, W.Y., Ch'ng, S.Y., Buys, Y.F. (2024). Graphene nanoplatelets/polylactic acid conductive polymer composites: tensile, thermal and electrical properties. Chemical Engineering & Technology, 47(11). https://doi.org/10.1002/ceat.202300592.
8. Mitchell, S., Low, J.H., Yoon, L.W. (2025). Oily wastewater remediation using polyurethane sponges coated with an optimised amount of graphene nanoplatelets. Asia-Pacific Journal of Science and Technology. https://doi.org/10.14456/apst.2026.1.
9. Kumarao, P., Ho, K.C., Hor Low, J., Leang Teh, J., Teow, Y.H. (2026). Study of antifouling Properties of MWCNTS/GNPS nanocomposite membrane against BSA protein. Journal of Engineering Science and Technology, 23(23rd EURECA 2025 Special Issue), 95-109.
10. Solouki, S., Karrabi, M., Eftekhari, M. (2024). Application of a functionalized thin-film composite nanofiltration membrane in water desalination. Journal of Molecular Liquids, 399, 124399. https://doi.org/10.1016/j.molliq.2024.124399.
11. Ho, K.C., Teow, Y.H., Ang, W.L., Mohammad, A.W. (2017). Novel GO/OMWCNTs mixed-matrix membrane with enhanced antifouling property for palm oil mill effluent treatment. Separation and Purification Technology, 177, 337-349. https://doi.org/10.1016/j.seppur.2017.01.014.
12. Avilés, F., Cauich-Rodríguez, J.V., Moo-Tah, L., May-Pat, A., Vargas-Coronado, R. (2009). Evaluation of mild acid oxidation treatments for MWCNT functionalization. Carbon, 47(13), 2970-2975. https://doi.org/10.1016/j.carbon.2009.06.044.
13. Datsyuk, V., Kalyva, M., Papagelis, K., Parthenios, J., Tasis, D., Siokou, A., Kallitsis, I., Galiotis, C. (2008). Chemical oxidation of multiwalled carbon nanotubes. Carbon, 46(6), 833-840. https://doi.org/10.1016/j.carbon.2008.02.012.
14. Kah Chun, H., Lim, J.H., Mohd Idris, A.I., Teow, Y.H., Ng, N.C. (2023). Effect of diameter of carbon nanotubes in nanocomposite membrane for methyl orange dye removal. Journal of Applied Membrane Science & Technology, 27(1), 47-61. https://doi.org/10.11113/amst.v27n1.262.
15. Al Mgheer, T., H Abdulrazzak, F. (2016). Oxidation of multi-walled carbon nanotubes in acidic and basic Piranha mixture. Frontiers in Nanoscience and Nanotechnology, 2(4). https://doi.org/10.15761/FNN.1000127.
16. Yeow, A.T.H., Chan, M.K., Ong, C.S., Ho, K.C. (2024). Effects of hydrogen bond donors on PVDF membrane modification using choline chloride-based deep eutectic solvents. Journal of Industrial and Engineering Chemistry. https://doi.org/10.1016/j.jiec.2024.05.028.
17. Lee, C.Z., Kah Chun, H., Chan, M.K., Teow, Y.H. (2022). Effect of carbon nanomaterials concentration in nanocomposite membrane for methyl blue dye removal. Jurnal Teknologi, 84(6), 19-27. https://doi.org/10.11113/jurnalteknologi.v84.18277.
18. Chan, M.K., Ong, C.S., Kumaran, P. (2018). Development and characterization of glycerol coating on the PAN/PVDF composite membranes. IOP Conference Series: Materials Science and Engineering, 458, 012006. https://doi.org/10.1088/1757-899X/458/1/012006.
19. Yadav, M., Upadhyaya, S., Singh, K. (2024). Preparation and characterization of PVDF Flat sheet membrane for VMD: Effect of different non-solvent additives and solvents in dope solution. Membrane and Water Treatment, 15(4), 163-176. https://doi.org/10.12989/mwt.2024.15.4.163.
20. Supelco Analytical Products (2022), Analytical procedures appendices Spectroquant® Prove Spectrophotometer 300; Merck KGaA, Darmstadt, Germany. https://www.sigmaaldrich.com/deepweb/assets/sigmaaldrich/product/documents/140/675/173017ug-en-ap-mk.pdf.
21. TN100 Turbidimeter Instruction Manual (2013), TN-100/T-100 portable turbidimeter instruction manual; Eutech Instruments Pte Ltd/Oakton Instruments, Ayer Rajah Crescent, Singapore/Vernon Hills, USA. https://www.eutechinst.com/manuals/english/waterproof_handheld/68X357701-TN100EC_r9.pdf.

22. Oakton 2700 Series Instruction Manual (2013), 2700 Series benchtop meters: pH 2700, ION 2700, CON 2700, DO 2700, PC 2700; Eutech Instruments Pte Ltd/Oakton Instruments, Ayer Rajah Crescent, Singapore/Vernon Hills, USA. https://pim-resources.coleparmer.com/instruction-manual/oak2700.pdf.
23. Hanna Instruments pH 210–213 Instruction Manual (1999), Microprocessor-based bench pH/mV/°C meters: models pH 210, pH 211, pH 212, pH 213; Hanna Instruments, Woonsocket, RI, USA. https://www.transcat.com/media/pdf/pH_210_11_12_13.pdf.
24. Ho, K.C., Raffi, S.M., Teow, Y.H. (2022). Synthesis of MWCNTs/TiO_2 photocatalytic nanocomposite membrane via in-situ colloidal precipitation method for methyl orange removal. International Journal of Nanoelectronics and Materials, 15(3), 207-222.
25. Kadhom, M., Albayati, N., Sultan, A.E., Al-Obaidi, M.A., Salih, S., Deng, B. (2025). Thin film nanocomposite (TFN) membranes filled with a novel metal organic framework for reverse osmosis applications. Membrane and Water Treatment, 16(3), 121-132. https://doi.org/10.12989/mwt.2025.16.3.121.
26. Sayed, E.S., Shaalan, H.F., Marzouk, M.I., Hani, H.A. (2024). Characterization and performance of post treated PVDF hollow fiber membrane. Membrane and Water Treatment, 15(2), 79-88. https://doi.org/10.12989/mwt.2024.15.2.079.
27. Goh, T.W., Ho, K.C., Teow, Y.H., McGarry, K. (2023). Influence of rGO/MWCNTs on antifouling properties of nanocomposite membrane: statistical analysis. 020014. https://doi.org/10.1063/5.0165317.
28. Sawant, S.R., Kalla, S., Murthy, Z.V.P. (2023). Enhanced properties of the PVDF membrane with carboxylated MWCNT and sodium alginate for membrane distillation. Journal of Environmental Chemical Engineering, 11(2), 109259. https://doi.org/10.1016/j.jece.2022.109259.
29. Wang, W., Xu, X., Zhang, Z., Zhang, P., Shi, Y., Ding, P. (2021). Study on the improvement of PVDF flat ultrafiltration membrane with MWCNTs-OH as the additive and the influence of different MWCNTs-OH scales. Colloid and Interface Science Communications, 43, 100433. https://doi.org/10.1016/j.colcom.2021.100433.
30. Tocoglu, U., Alaf, M., Cevher, O., Guler, M.O., Akbulut, H. (2012). The effect of oxidants on the formation of multi-walled carbon nanotube buckypaper. Journal of Nanoscience and Nanotechnology, 12(12), 9169-9174. https://doi.org/10.1166/jnn.2012.6751.
31. Shah, P., Murthy, C.N. (2013). Studies on the porosity control of MWCNT/polysulfone composite membrane and its effect on metal removal. Journal of Membrane Science, 437, 90-98. https://doi.org/10.1016/j.memsci.2013.02.042.
32. Xu, T., Qi, Z., Tan, Y., Tian, J., Li, X. (2021). Effect of multiwalled carbon nanotube diameter on mechanical behavior and fracture toughness of epoxy nanocomposites. Materials Research Express, 8(1), 015014. https://doi.org/10.1088/2053-1591/abd864.
33. Gholami, S., Llacuna, J. L., Vatanpour, V., Dehqan, A., Paziresh, S., Cortina, J.L. (2022). Impact of a new functionalization of multiwalled carbon nanotubes on antifouling and permeability of PVDF nanocomposite membranes for dye wastewater treatment. Chemosphere, 294, 133699. https://doi.org/10.1016/j.chemosphere.2022.133699.
34. Zahedipoor, A., Faramarzi, M., Mansourizadeh, A., Ghaedi, A., Emadzadeh, D. (2023). Integration of porous nanomaterial-infused membrane in UF/FO membrane hybrid for simulated osmosis membrane bioreactor (OsMBR) process. Membranes, 13(6). https://doi.org/10.3390/membranes13060577.
35. He, M., Zhang, S., Su, Y., Zhang, R., Liu, Y., Jiang, Z. (2018). Manipulating membrane surface porosity and pore size by in-situ assembly of Pluronic F127 and tannin. Journal of Membrane Science, 556, 285-292. https://doi.org/10.1016/j.memsci.2018.03.087.
36. Xie, Y., Yu, L., Yu, Y. (2024). Improved desalination performance of fluorinated graphene oxide blended PVDF electrospun nanofiber membrane for air gap membrane distillation. Desalination and Water Treatment, 317, 100184. https://doi.org/10.1016/j.dwt.2024.100184.
37. Hamad, M.E., Al-Gharabli, S., Kujawa, J. (2022). Tunable hydrophobicity and roughness on PVDF surface by grafting to mode - Approach to enhance membrane performance in membrane distillation process. Separation and Purification Technology, 291, 120935. https://doi.org/10.1016/j.seppur.2022.120935.

38. Zhu, M., Mao, Y. (2020). Large-pore-size membranes tuned by chemically vapor deposited nanocoatings for rapid and controlled desalination. RSC Advances, 10(66), 40562-40568. https://doi.org/10.1039/D0RA07629E.
39. Muzemder, A.S.H., Singh, K. (2024). Influence of sedimentary structure and pore-size distribution on upscaling permeability and flow enhancement due to liquid boundary slip: A pore-scale computational study. Advances in Water Resources, 190, 104752. https://doi.org/10.1016/j.advwatres.2024.104752.
40. Chen, Y.M., Kah Chun, H., Chan, M.K., Teow, Y.H., Aida Isma, M. (2022). Optimization of antifouling properties of mixed matrix membrane synthesized via in-situ colloidal precipitation. Journal of Membrane Science and Research.
41. Silva, E.A. da, Windmöller, D., Silva, G.G., Figueiredo, K.C.S. (2017). Polydimethylsiloxane membranes containing multi-walled carbon nanotubes for gas separation. Materials Research, 20(6), 1454-1460. https://doi.org/10.1590/1980-5373-mr-2016-0825.
42. Chen, M., Rietveld, L.C., Heijman, S.G.J. (2025). Evaluation of membrane fouling at constant flux and constant transmembrane pressure conditions: implications for membrane modification. Journal of Environmental Chemical Engineering, 13(5), 117823. https://doi.org/10.1016/J.JECE.2025.117823.
43. Hilal, N., Al-Zoubi, H., Darwish, N.A., Mohamma, A.W., Abu Arabi, M. (2014). A comprehensive review of nanofiltration membranes: treatment, pretreatment, modelling, and atomic force microscopy. Desalination, 170(3), 281-308. https://doi.org/10.1016/j.desal.2004.01.007.
44. Sultana, N., Roddick, F.A., Pramanik, B.K. (2024). Fat, oil and grease wastewater and dishwashers: uncovering the link to fog deposition. Science of The Total Environment, 907, 168032. https://doi.org/10.1016/j.scitotenv.2023.168032.
45. Ramon, G.Z., Hoek, E.M.V. (2012). On the enhanced drag force induced by permeation through a filtration membrane. Journal of Membrane Science, 392-393, 1-8. https://doi.org/10.1016/J.MEMSCI.2011.10.056.
46. Mahlangu, O.T., Nthunya, L.N., Motsa, M.M., Morifi, E., Richards, H., Mamba, B.B. (2023). Fouling of high pressure-driven NF and RO membranes in desalination processes: mechanisms and implications on salt rejection. Chemical Engineering Research and Design, 199, 268-295. https://doi.org/10.1016/j.cherd.2023.09.037.
47. Chang, I.S., Bag, S.O., Lee, C.H. (2001). Effects of membrane fouling on solute rejection during membrane filtration of activated sludge. Process Biochemistry, 36(8-9), 855-860. https://doi.org/10.1016/S0032-9592(00)00284-3.
48. Kamaruddin, M.A., Ibrahim, M.H., Thung, L.M., Emmanuel, M.I., Niza, N.M., Shadi, A.M.H., Norashiddin, F.A. (2019). Sustainable synthesis of pectinolytic enzymes from citrus and Musa acuminata peels for biochemical oxygen demand and grease removal by batch protocol. Applied Water Science, 9(4), 68. https://doi.org/10.1007/s13201-019-0948-2.
49. Pandey, A., Qamar, S. F., Das, S., Basu, S., Kesarwani, H., Saxena, A., Sharma, S., Sarkar, J. (2024). Advanced multi-wall carbon nanotube-optimized surfactant-polymer flooding for enhanced oil recovery. Fuel, 355, 129463. https://doi.org/10.1016/j.fuel.2023.129463.
50. Wang, Z., Liu, Q., Yan, P., Zhang, J., Liang, X., Ma, X., Li, J., Cui, Z. (2025). Regulation of the microstructure for hollow fiber ultrafiltration membrane with “flocculation” effect and study on the mechanism of “adsorption flocculation-loose cake layer protection” against humic acid fouling. Journal of Water Process Engineering, 69, 106697. https://doi.org/10.1016/j.jwpe.2024.106697.
51. Jan, A., Nijboer, M., Qin, G., Luiten-Olieman, M., Rietveld, L. C., Heijman, S. G. J. (2025). Silicon carbide coated alumina tight-ultrafiltration membrane prepared by low-pressure chemical vapor deposition for sulphate ion retention. Desalination, 613, 119085. https://doi.org/10.1016/J.DESAL.2025.119085.
52. Alborzi, A., Hsieh, I.M., Reible, D., Malmali, M. (2022). Analysis of fouling mechanism in ultrafiltration of produced water. Journal of Water Process Engineering, 49, 102978. https://doi.org/10.1016/j.jwpe.2022.102978.
53. Younas, H., Ur Rehman Afridi, Z., Zhou, Y., Cui, Z. (2020). Progress and perspective of antifouling, pressure driven, flat-sheet nanocomposite, polymeric membranes in water treatment. Journal of

Membrane Science and Research, 6(3), 319-332. https://doi.org/10.22079/JMSR.2020.117983.1312.
54. Al-Sammarraie, E.S.A., Sabirova, T.M., Meskher, H., Al-Juboori, R.A., Zyryanov, G.V., Alsalhy, Q.F. (2025). Nanocomposite UF membrane of PVC/nano-silica modified with SDS for carwash wastewater treatment. Environmental Science: Advances, 4(3), 469-488. https://doi.org/10.1039/D4VA00088A.
55. Abumounshar, N., Pandey, R.P., Hasan, S.W. (2024). Enhanced hydrophilicity and antibacterial efficacy of in-situ silver nanoparticles decorated $Ti_3C_2T_x$/Polylactic acid composite membrane for real hospital wastewater purification. Science of The Total Environment, 954, 176697. https://doi.org/10.1016/j.scitotenv.2024.176697.